

# Small scale WIMP physics

Anne M. Green\*, Stefan Hofman† and Dominik J. Schwarz\*\*

\**Physics and Astronomy, University of Sheffield, Sheffield S3 7RH, UK*

†*Perimeter Institute for Theoretical Physics, Waterloo, Ontario, N2L2Y5, Canada*

\*\**Fakultät für Physik, Universität Bielefeld, Postfach 100131, 33501 Bielefeld, Germany*

## Abstract.

The dark matter distribution on small scales may depend on the properties of the first generation of dark matter halos to form, which is in turn determined by the microphysics of the dark matter particles. We overview the microphysics of WIMPs and our calculations of the collisional damping and free streaming scales. We then plot the resulting density perturbation power spectrum and red-shift at which typical halos form, taking into account the effect of uncertainties in the WIMP properties (mass and interaction channel) and the primordial power spectrum. Finally we review recent developments regarding the properties and fate of the first WIMPy halos.

**Keywords:** dark matter, cosmological perturbation theory

**PACS:** 95.35.+d, 95.30.Cq, 98.35.Gi

## WHY?

Diverse cosmological observations indicate that the Universe contains a significant amount of non-baryonic cold dark matter (CDM). Weakly interacting massive particles (WIMPs) are an attractive CDM candidate, as a stable relic from the electroweak scale generically has an interesting present day density,  $\Omega_{\text{cdm}} \sim \mathcal{O}(1)$ .

According to standard lore the distribution of CDM is independent of its nature (WIMPs, axions, or something more exotic). This is true on large (super-kpc) scales, but may not be the case on small (sub-pc) scales. Furthermore the signals expected in WIMP detection experiments depend on the dark matter distribution. WIMP direct detection experiments (which aim to detect WIMPs in the lab via their elastic scattering off detector nuclei) probe the dark matter distribution on sub-milli-pc scales. WIMP indirect detection involves searching for the products ( $\gamma$ -rays, antiprotons and neutrinos) of WIMP annihilation and, since this is a two-body process, the event rates are proportional to the density squared and are hence enhanced by substructure. Reliable predictions for the expected signals therefore require an understanding of the distribution of dark matter on small (sub-galactic) scales.

In CDM cosmologies structure forms hierarchically; small halos form first with larger halos forming via mergers and accretion. The density perturbations on very small scales, and hence the properties of the first generation of structures to form, depend on the micro-physics of the CDM and the present day density distribution may retain traces of these first structures.

## WIMP MICRO-PHYSICS

In the early Universe WIMPs are kept in thermal equilibrium with the radiation component via chemical interactions. As the Universe expands the WIMP density decreases, these interactions cease and the WIMPs chemically decouple or ‘freeze-out’. After this the WIMP comoving number density remains constant, however WIMPs continue to interact kinetically, via elastic scattering, with the radiation component and are kept in local thermal equilibrium. Eventually the WIMP density becomes so low that elastic scattering ceases and the WIMPs kinetically decouple. The average momentum exchanged per collision is small however [1] so the relaxation timescale, which characterises the time at which WIMPs kinetically decouple, is significantly larger than the elastic scattering timescale. While chemical decoupling happens at a temperature  $T_{\text{cd}} \sim \mathcal{O}(10 \text{ GeV})$ , kinetic decoupling is delayed by the large entropy of the hot Universe and takes place at a temperature  $T_{\text{kd}} \sim \mathcal{O}(10 \text{ MeV})$ . This is generic for any WIMP that is of cosmological relevance today.

Elastic scattering processes around  $T_{\text{kd}}$  lead to viscous coupling of the WIMP and radiation fluids, resulting in collisional damping of WIMP perturbations due to bulk and shear viscosity [1]. The collisional damping scale was first derived in Ref. [1] by two of the present authors, and we presented a more intuitive, but less rigorous, derivation using the linearised Navier-Stokes equation in Ref. [2]. The net result is exponential damping with a characteristic wave-number

$$k_{\text{d}} = \frac{3.76 \times 10^7}{\text{Mpc}} \left( \frac{m}{100 \text{ GeV}} \right)^{1/2} \left( \frac{T_{\text{kd}}}{30 \text{ MeV}} \right)^{1/2}, \quad (1)$$

where  $m$  is the WIMP mass.

One caveat is that our treatment is restricted to sub-horizon scales. Near the horizon there are additional effects, which have recently been studied numerically by Loeb and Zaldarriaga [3]. Their results confirm that the essential features of the subhorizon damping are captured by our calculation, but the additional terms play an important role in determining the precise position of the maximum of the CDM power spectrum. We agree with their conclusion that an accurate calculation (better than 10% accuracy) must be based on a numerical computation including all of the terms.

After kinetic decoupling the WIMPs free-stream and their distribution function is governed by the collisionless Boltzmann equation. We study the subsequent additional damping by considering small perturbations away from the local thermal equilibrium solution, taking into account the perturbations present at kinetic decoupling. The characteristic free-streaming scale becomes constant after matter-radiation equality and is given by

$$k_{\text{fs}} = \frac{1.70 \times 10^6}{\text{Mpc}} \frac{(m/100 \text{ GeV})^{1/2} (T_{\text{kd}}/30 \text{ MeV})^{1/2}}{1 + \ln(T_{\text{kd}}/30 \text{ MeV})/19.2}. \quad (2)$$

The free streaming leads to exponential damping of the WIMP density contrast again but with an additional polynomial pre-factor [4, 2]. Since  $k_{\text{fs}} < k_{\text{d}}$ , the cut-off in the power spectrum is determined by the free streaming scale  $k_{\text{fs}}$ .

We focus on four benchmark models which span the range of most plausible WIMP properties and have present day densities in accordance with the WMAP measurement of the cold dark matter density. The details of these benchmark models, including the values of  $k_{\text{d}}$  and  $k_{\text{fs}}$ , are tabulated in Table 1.  $l$  parameterises the temperature dependence of the thermally averaged elastic scattering cross section:  $\langle \sigma_{\text{el}} \rangle = \sigma_0^{\text{el}} (T/m)^{1+l}$ . In the Standard Model, elastic scattering between a light fermion and a heavy fermion is mediated by  $Z^0$  exchange and  $l = 0$ . Other channels may occur however. In supersymmetric extensions of the Standard Model, where the lightest neutralino is a WIMP candidate, sfermion exchange occurs (and if the neutralino is a gaugino,  $Z^0$  exchange is suppressed), in which case  $l = 1$ . Models B and C are very close to the bino-like neutralino case considered in Ref. [4]. Models A and D show that there is more spread in the predicted damping scale if the assumption of a bino-like WIMP is dropped.

## POWER SPECTRUM AND $Z_{\text{NL}}$

The (processed) power spectrum depends on two more ingredients: the gravitational growth of perturbations and the primordial power spectrum. We calculate the trans-

fer function, which encodes the gravitational growth, by solving the equations which govern the evolution of perturbations in matter and radiation fluids during two overlapping epochs, radiation domination and close to matter-radiation equality, and then matching these solutions together (see Ref. [2] for further details). We neglect perturbations in the baryon fluid. This approximation is valid on small scales  $k > k_{\text{b}} \sim 10^3 \text{ Mpc}^{-1}$  for  $z > z_{\text{b}} \sim 150$ . We have verified that our analytic expressions are accurate at the 10% level by comparing them with the output of the COSMICS package. This is sufficient given current uncertainties in the cosmological parameters and the primordial power spectrum.

The resulting linear power spectrum, defined as  $\mathcal{P}_{\Delta}(k, z) = k^3/(2\pi^2) \langle |\Delta(k, z)|^2 \rangle$ , at  $z = 300$  (before the onset of non-linear structure formation) is plotted in the left panel in Fig. 1 for our benchmark WIMP models and a WMAP normalised scale-invariant primordial power spectrum. The characteristic free-streaming wave-number is smallest for model A (Dirac WIMP with  $l=0$ ) and increases with increasing mass for the Majorana WIMPs (models B-D). This is clearly reflected in the position of the cut-off in the power spectrum in Fig. 1.

The cut-off in the WIMP power spectrum sets the scale of the first halos to form. We estimate the redshift at which typical (1- $\sigma$ ) fluctuations on comoving scale  $R$  go nonlinear via  $\sigma(R, z_{\text{nl}}) = 1$ , where  $\sigma(R, z)$  is the mass variance defined by

$$\sigma^2(R, z) = \int_0^\infty W^2(kR) \mathcal{P}_{\Delta}(k, z) \frac{dk}{k}, \quad (3)$$

where  $W(kR)$  is the Fourier transform of the window function, which we take to be a top hat, divided by its volume.

The right panel of Fig. 1 shows  $z_{\text{nl}}$  as a function of scale  $R$ . The cut-off in the processed power spectrum at  $k \sim 10^6 \text{ Mpc}^{-1}$  leads to a plateau with  $z_{\text{nl}} = z_{\text{nl}}^{\text{max}}$  at  $R < R_{\text{min}} = \mathcal{O}(1) \text{ pc}$ . We emphasise that  $z_{\text{nl}}^{\text{max}}$  is the redshift at which hierarchical structure formation starts at a typical place in the universe, the very first WIMPy halos will form significantly earlier from rare large fluctuations. The order of magnitude variation in  $k_{\text{fs}}$  leads to a similar variation in  $R_{\text{min}}$  and also (because of the dependence of the amplitude of the peak of the power spectrum on the cut-off scale) a range of values  $z_{\text{nl}}^{\text{max}} \approx 50$  to 65.

We now turn our attention to the effect of the uncertainty in the primordial power spectrum. On the scales probed by the CMB [ $\mathcal{O}(0.01 - 0.1) \text{ Mpc}^{-1}$ ] the primordial power spectrum is close to scale invariant. The free-streaming scale  $k_{\text{fs}} \sim 10^6 \text{ Mpc}^{-1}$  is seven orders of magnitude smaller and therefore even a very small scale dependence of the power spectrum could significantly change the amplitude of the power spectrum at the cut-off scale, and hence the red-shift at which the first WIMP

**TABLE 1.** Benchmark WIMP models.

Ref.	$l$	$m$ (GeV)	$T_{cd}$ (GeV)	$T_{kd}$ (Mev)	$k_d$ (pc $^{-1}$ )	$k_{fs}$ (pc $^{-1}$ )
A	0	100	3.6	1.6	14	0.42
B	1	50	1.9	21	39	0.94
C	1	100	3.7	25	61	1.5
D	1	500	17	37	180	4.0

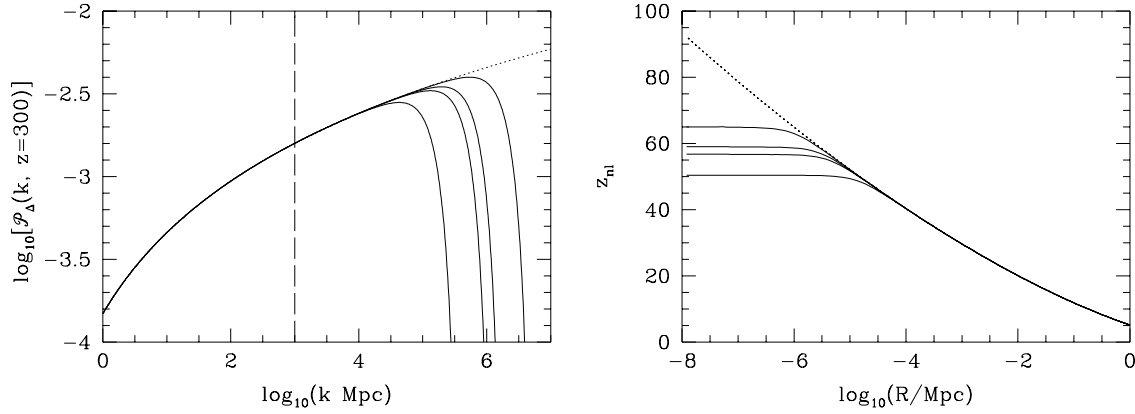


**FIGURE 1.** The processed power spectrum at  $z = 300$ ,  $\mathcal{P}_\Delta(k, z = 300)$ , (left) and the red-shift at which  $1 - \sigma$  fluctuations go non-linear,  $z_{nl}$ , (right) for a WMAP normalised scale-invariant primordial power spectrum and from left to right/bottom to top a Dirac WIMP with  $m = 100$  GeV and Majorana WIMPs with  $m = 50, 100, 500$  GeV. Without the effects of collisional damping and free streaming these quantities would be given by the dotted line. The vertical dashed line denotes  $k_b$ , the wavenumber below which baryons follow CDM. Our approximations are optimised for  $k > k_b$ .

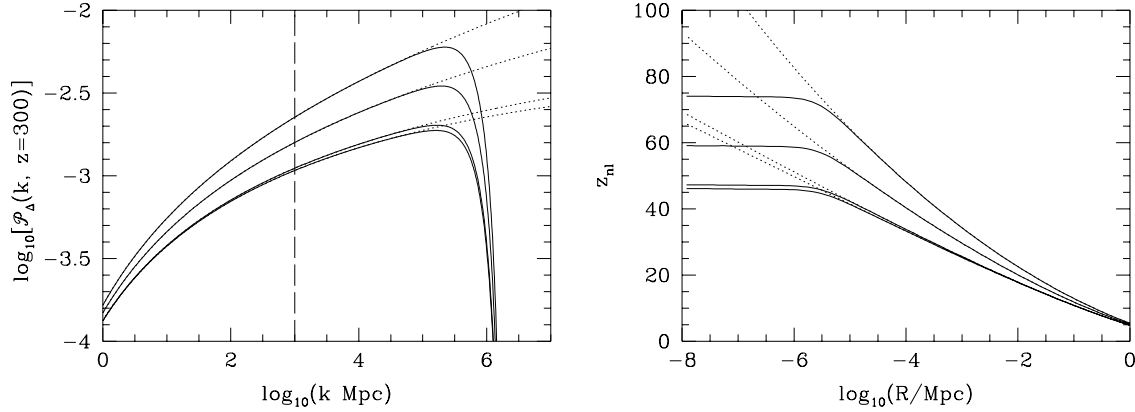


**FIGURE 2.** As Fig. 1 for WIMP benchmark model C (a bino like WIMP with  $m = 100$  GeV) and from top to bottom false vacuum dominated hybrid inflation ( $n = 1.036, \alpha = 0$ ), a scale invariant primordial power spectrum ( $n = 1, \alpha = 0$ ), power law inflation ( $n = 0.964, \alpha = 0$ ) and  $m^2\phi^2$  chaotic inflation ( $n = 0.964, \alpha = -0.0006$ ).

halos form. The most commonly used parameterisation of the primordial power spectrum is

$$\mathcal{P}(k) = \mathcal{P}(k_0) \left( \frac{k}{k_0} \right)^{n(k_0) - 1 + \frac{1}{2}\alpha(k_0)\ln(k/k_0)}, \quad (4)$$

where  $\alpha(k) = dn/dk$ . The spectral index  $n$  and its running  $\alpha$  depend on the inflationary potential.

To assess the effects of possible scale dependence of the primordial power spectrum we consider three benchmark inflation models which span the range of possible power spectra for simple inflation models:  $V = m^2\phi^2$  chaotic inflation, with  $N = 55$  e-foldings of inflation so that  $n - 1 = -0.036$  and  $\alpha = -6 \times 10^{-4}$ , power law inflation ( $a \propto t^p$ ), with  $p = 55.4$  so that  $n - 1 = -0.036$ , to match the chaotic inflation model, but in this case  $\alpha = 0$  and false vacuum dominated hybrid inflation with the largest spectral index allowed by the WMAP data,  $n - 1 = 0.036$  and  $\alpha = 0$ . For further details see Sec. 7 of Ref. [2].

The amplitude of the primordial power spectra on the free-streaming scale  $\sim 10^6 \text{Mpc}^{-1}$  varies by a factor of  $\sim 2.5$  (equivalently the amplitude of the fluctuations varies by  $\sim \sqrt{2.5} \sim 1.6$ ). The resulting processed power spectra and the red-shift at which scales go non-linear are plotted in Fig.2 for a Majorana WIMP with  $m = 100 \text{GeV}$ . The variation in the amplitude of the primordial power spectra at the cut-off scale translates directly into a variation in the peak amplitude of the processed power spectra and hence  $z_{\text{nl}}^{\text{max}}$ .

## PROPERTIES AND FATE OF THE FIRST HALOS

We estimate the size and mass of the first generation of typical subhalos that form at  $z_{\text{nl}}^{\text{max}}$  using the spherical collapse model [4, 2]. The mean CDM mass within a sphere of comoving radius  $R$  is  $M(R) = 1.6 \times 10^{-7} M_{\odot} (R/\text{pc})^3$ , with over-densities having twice this mass. The present day radius, after turn-around and violent relaxation, would be of order tens of milli-pc, comparable to the size of the solar system, and smaller.

Numerical simulations are required to study the detailed properties, and fate, of the first generation of WIMP halos to form. Diemand et al. [5] have recently published the results of the first such simulations to be carried out. They use a multi-scale technique to study the non-linear collapse of a small,  $(60 \text{ comoving pc})^3$ , average density region starting at  $z = 350$ . The first non-linear structures form at  $z \sim 60$  and have  $M \sim 10^{-6} M_{\odot}$ , in good agreement with our analytic calculations. The simulations have to be stopped at  $z \sim 25$  when the high resolution region begins to merge with the surrounding lower resolution regions.

These mini-halos are subsequently subject to a number of dynamical processes which could destroy them. Matter will be tidally stripped from the outer regions if the gravitational force of the parent halo exceeds that of the sub-halo. Diemand et al. estimate that the mini halos should not be tidally destroyed outside the inner few parsecs of the Milky Way [5], in contrast to earlier analytic calculations by Berezhinsky et al. [6]. The mini-halos can also be destroyed via interactions with compact objects. Zhao et al. argue that encounters with stars destroy all of the mini halos in the solar neighbourhood [7], Moore et al. however disagree [8]. Further numerical simulations of the dynamical evolution and interactions of mini-halos are probably required to resolve these issues.

## SUMMARY

WIMP direct and indirect detection both probe the dark matter distribution on small scales, which depends on the properties, and hence fate, of the first generation of WIMP halos to form. Collisional damping and free-streaming erase density perturbations on small scales ( $k > 10^6 \text{Mpc}^{-1}$ ) and set the scale of the first generation of WIMP halos to form ( $M \sim 10^{-6} M_{\odot}$ ). The fate of these halos, specifically whether or not a significant fraction survive to the present day within the Milky Way, remains an open question.

## ACKNOWLEDGMENTS

AMG is supported by PPARC.

## REFERENCES

1. S. Hofmann, D. J. Schwarz and H. Stöcker, Phys. Rev. D **64**, 083507 (2001) [astro-ph/0104173]
2. A. M. Green, S. Hofmann and D. J. Schwarz, JCAP **08**, 003 (2005) [astro-ph/0503387]
3. A. Loeb and M. Zaldarriaga, Phys. Rev. D **71**, 103520 (2005) [astro-ph/0504112]
4. A. M. Green, S. Hofmann and D. J. Schwarz, Mon. Not. Roy. Astron. Soc. **353**, L23 (2004) [astro-ph/0309621]
5. J. Diemand, B. Moore and J. Stadel, Nature **433**, 389 (2005) [astro-ph/0501589]
6. V. Berezhinsky, V. Dokuchaev and Y. Eroshenko, Phys. Rev. D **68** 103003 (2003) [astro-ph/0301551]
7. H. Zhao, J. E. Taylor, J. Silk and D. Hooper [astro-ph/0502049]; [astro-ph/0508215]
8. B. Moore, J. Diemand, J. Stadel and T. Quinn [astro-ph/0502213]